XX IMEKO World Congress
Metrology for Green Growth
September 9–14, 2012, Busan, Republic of Korea

FABRICATION AND CHARACTERIZATION OF FERROELECTRIC POLY (VINYLIDENE FLUORIDE -*CO*-TRIFLUOROETHYLENE) NANODOTS

Yoon-Young Choi,[1] *Moonkyu Park*[1], *Jongin Hong*[2], *and Kwangsoo No*[1†]

[1]*Department of Materials Science and Engineering, KAIST, Daejeon 305-701, Republic of Korea*
[2]*Center for Mass and related quantities, Division of Physical Metrology, KRISS, Daejeon 305-340, Republic of Korea*
[3]*Department of Chemistry, Chung-Ang University, Seoul 156-756, Republic of Korea*
E-mail address:yychoi@kaist.ac.kr

Abstract: We demonstrated a facile route to fabricate ferroelectric poly(vinylidene fluoride-trifluoroethylene), P(VDF-TrFE), nanodots from spin-coated thin films. Importantly, the discrete P(VDF-TrFE) nanodots possessed high degree of β-phase [F(β) > 60%] when compared to the fraction of β-phase in thin films [F(β) = 51%]. P(VDF–TrFE) nanodots of 51.4 ± 10.6 nm in height and 172.75 ± 40.5 nm in diameter displayed superior piezoresponse values (18.1 ± 3.3 pm/V) and a low coercive voltage (2.4 ± 0.5V). This offers our rationale for a great promise in non-volatile memories, infrared sensor arrays and artificial skin applications.

Keywords: Ferroelectric P(VDF-TrFE) nanodots, Spin coating, Dewetting, Piezoresponse force microscopy

INTRODUCTION

Ferroelectric and piezoelectric nanostructures have attracted much interest for potential applications in miniaturized sensor arrays, actuators and non-volatile memory devices. Recently, it is reported that piezoelectric properties of nanostructured ferroelectric materials are superior to those of their bulk counterparts because their lateral size confinement would allow for homogenous nucleation.[1–5] Accordingly, there have been many efforts made to fabricate various ferroelectric nanostructures. Several research groups have successfully developed one-dimensional or quasi-zero dimensional nanostructures in this range using both lithographic[6,7] ("top-down") and self-assembly methods[8–10] ("bottom-up"). The former method is well-suited to the fabrication of regular arrays of ferroelectric nanostructures, but their surfaces can be damaged during the harsh processing conditions and the whole process is laborious.[11,12] In contrast, self-assembly is an effective method for producing nanoscale structures not only because of its simplicity and the inexpensive cost of processing under mild conditions, but also because of its potential to overcome the size limitations of the conventional top down process.[13,14] Among various ferroelectric materials, poly(vinylidene fluoride–trifluoroethylene) P(VDF–TrFE), is a prime candidate for ferroelectric nanodevices because of its large remnant polarization, short switching time and good thermal stability.[11-15] High flexibility, low weight, inexpensive processing techniques, and easy modification of shape and size, are also primary advantages of this ferroelectric polymer.[15,16] However, its coercive field is approximately 50 MV/m, which is much higher than that of ferroelectric oxide materials.[11] Although reducing the film thickness of a ferroelectric layer below 100 nm allows for low operating voltage to be used,[17–19] decreasing the film thickness results in deterioration of the ferroelectric properties due to the reduction of crystallinity and crystallite size.[11] However, it is reported that nano-imprinted P(VDF–TrFE) nanostructures allowed for elimination of internal structural defects and improvement of crystal orientation in the nanostructures with a low coercive field of ~10 MV/m.[11] Recently, Ducharme *et al*. made self-assembled P(VDF–TrFE) nanomesas that were 9 nm in height and 100 nm in diameter from ultrathin Langmuir–Blodgett (LB) films after post-annealing.[9] This process has been exclusively utilized to fabricate self-assembled P(VDF–TrFE) nanostructures. It should be noted that the LB technique is a time consuming process. It is also difficult to fabricate fluorine-containing polymer films because of their rigidity and hydrophobicity. Accordingly, we propose a facile method for the fabrication of self-assembled P(VDF–TrFE) nanostructures. We successfully fabricated P(VDF–TrFE) nanodots by using a simple spin-coating technique with post-annealing, which is more suitable for applying to practical applications than the LB technique.

METHODS

P(VDF–TrFE) nanodots were fabricated by spin-coating and post-annealing processes. In this work, we used a molar ratio of 75/25 P(VDF–TrFE) copolymer, which is known to have good

piezoelectric properties. The P(VDF–TrFE) pellets (MSI Sensor, PA, USA) were dissolved in methyl ethyl ketone (MEK), and solutions with concentrations in the range 3 wt% to 0.25 wt% were prepared by sonication. The solutions with different concentrations were filtered using a 0.2 μm syringe filter and then spin coated onto the $Au/Ti/SiO_2$ substrates at 5000 rpm for 20 s. To produce the nanodots, the P(VDF–TrFE) films were immediately annealed at 150 ℃ for 2 hours on a hot plate. The initial thickness of the P(VDF–TrFE) films was measured using scanning electron microscopy (Hitachi, S-4800, Japan). The surface morphology of the films annealed at 150 ℃ was obtained using commercial atomic force microscopy (AFM, Seiko, SPA400, Japan) with a SiN tip (Olympus, force constant of 0.08 N/m and resonance frequency of 34 kHz). To determine the ferroelectric molecular conformations of the nanostructures, we utilized Fourier transform infrared (FT-IR) spectroscopy in attenuated total reflection (ATR) mode (Bruker, IFS66V/S & HYPERION 3000, Germany) with a scanning resolution of 2 cm^{-1}. Topography, amplitude and phase images were acquired simultaneously using the piezoresponse force microscopy (PFM) method using a commercial atomic force microscope (PSIA, XE-100, Korea) equipped with an external signal generation and data acquisition system. An ac modulation voltage of 0.8 V_{rms} at 17 kHz was applied to the AFM tip of Pt-coated Si cantilevers with a tip apex radius of 40 nm (Micromasch, spring constant $k \approx 6.0$ N/m) over a scan area of 2 × 2 μm^2. The local piezoelectric hysteresis loop was obtained at a fixed tip position during the dc voltage sweep.

RESULTS AND DISCUSSION

Fig. 1(b) shows AFM topographic images of the P(VDF–TrFE) films made with different concentrations of P(VDF-TrFE) solution and annealed at 150 ℃. As the film thickness decreased, the film morphology changed gradually from a continuous film to isolated nanodots. These observations may indicate that the formation of P(VDF–TrFE) nanostructures depends on the film thickness and that there exists a critical thickness (t < 24.03 ± 3.5 nm) at which nanostructures form in our study. We speculate that the formation of nanostructures in the ferroelectric P(VDF–TrFE) films might be attributed to the dewetting process. It is known that dewetting of polymer films is observed when thin liquid films (thickness < 100 nm) are annealed above the glass transition temperature (T_g). The mechanism of nanodot formation is mainly elucidated by a spinodal decomposition process based on amplification of thermal fluctuations on the surface of thin liquid films. In our case, the P(VDF–TrFE) film is unstable after deposition at room temperature because its glass transition temperature (T_g) is –36 ℃. Accordingly, the unstable P(VDF–TrFE) thin film would break up *via* the dewetting process in order to minimize the area where the P(VDF–TrFE) has contact with the substrate. The substrate surface is exposed and the film is laterally separated. Eventually, such nanodots are formed on the substrate. To understand the formation mechanism of the nanostructures, we also investigated the dependence of surface morphology on film thickness by changing the annealing temperature . We observed that the formation temperature of P(VDF–TrFE) nanostructures decreased with decreasing initial film thickness. Of special significance were the observations that at a film thickness of 10.45 ± 1.4 nm, a morphological transition from continuous film to nanodots was found when the annealing temperature was raised from 120 to 130 ℃ and that the nanodots were formed up to annealing temperature of 150 ℃. We speculate that these observations might be also associated with the dewetting mechanism in P(VDF–TrFE) thin films. The dewetting of the P(VDF–TrFE) films took place when the P(VDF–TrFE) thin films (t < 24.03 ± 3.5 nm) were heated to a high enough temperature for the film morphology to rearrange due to the increase in molecular mobility. The conformation characterization of the P(VDF–TrFE) nanostructures was investigated using FT-IR spectroscopy. In Fig. 2, the absorption bands at 1290 cm^{-1} and 848 cm^{-1} (A_1, $\boldsymbol{\mu} \parallel \boldsymbol{b}$) are associated with the β-phase possessing *trans* sequences longer than 4 monomers (t_m > 4) and *trans* sequences longer than 3 monomers (t_m > 3), respectively. The 885 cm^{-1} peak (B_2, $\boldsymbol{\mu} \parallel \boldsymbol{a}$) is related to the β-phase having a *trans* sequence of one monomer. These three peaks can be used for evaluating the ferroelectric crystalline β-phase of the nanodots. Meanwhile, the absorbance bands at 612 cm^{-1} and 802 cm^{-1} correspond to the α-phase possessing the *trans–gauche* (TG) conformation. Assuming that the FT-IR absorption follows the Beer–Lambert law, the fraction of β-phase F(β) in the nanodots can be calculated using equation (1)[17]:

$$F(\beta) = \frac{m_\beta}{m_\alpha + m_\beta} = \frac{A_\beta}{1.26A_\alpha + A_\beta} \quad (1)$$

where m is the mass of the α and β phases, and A is the absorbance of the α and β phases with absorbance peaks at 612 cm^{-1}, 1292 cm^{-1}, respectively.[17,31] All the P(VDF–TrFE) nanodots showed high contents of β-phase over 53% (Table 1), compared with a β-phase fraction of 51% for 900nm thick stretched P(VDF–TrFE) film.[17] This result indicates that the ferroelectric β-phase is better formed in the P(VDF–TrFE) nanodots than the P(VDF–TrFE) films. We believe that the lateral size confinement of the P(VDF–TrFE) nanodots might affect the nucleation mechanism and the crystallographic orientations.[4,5]

Fig. 3(a) shows AFM topographic images of the P(VDF–TrFE) nanodots. The 24.03 ± 3.5 nm thick films changed to nanodots with average diameters of 1072 ± 613 nm and thicknesses of 95.57 ± 35.4 nm. The 17.93 ± 2.0 nm thick films produced slightly smaller nanodots with average diameters of 504 ± 244

nm and thicknesses of 82.85 ± 11.2 nm. The 10.45 ± 1.4 nm thick film showed completely isolated nanodots with average diameters of 172.75 ± 40.5 nm and thicknesses of 51.4 ± 10.6 nm. We observed that the size of the nanodots decreased as the initial film thickness reduced. Moreover, the isolated nanodots showed very uniform size distribution. Fig. 3 shows both the topography and piezoresponse images of the P(VDF–TrFE) nanodots obtained from different initial film thicknesses. In the PFM amplitude images, the bright regions represent the domains showing relatively strong piezoelectric properties, while the dark regions indicate areas which do not show piezoelectric properties. In the PFM phase images, bright regions correspond to domains with polarization directed towards the sample surface, whilst dark regions show domains with polarization directed towards the substrate. Strong amplitude and phase signals were observed at the position of the nanostructures in the topographic images. This indicates that the P(VDF–TrFE) nanostructures showed superior piezoelectric properties. Interestingly, all the nanodots showed dark phase contrast images [Fig. 3(c)]. This indicates that the spontaneous polarizations in P(VDF–TrFE) nanostructures would be self-oriented towards the downwards direction. Details about the self-alignment in the P(VDF-TrFE) nanodots are beyond the scope of this study. However, it might be related to the film fabrication process, *i.e.* the spin coating process, in which an induced elongation force facilitates direct formation of the β-phase in the P(VDF–TrFE) film. In addition, the self-alignment might be a result of the lateral size confinement of the P(VDF-TrFE) nanodots, which permits homogenous nucleation of crystalline phases.[4,5] In order to investigate the polarization switching properties of the P(VDF–TrFE) nanodots, we measured local piezoresponse hysteresis loops at ten randomly selected points and averaged them (Fig. 4.) As expected, the P(VDF–TrFE) nanodots showed a superior d_{33} value (d_{33} =18.1 ± 3.3 pm/V) and low coercive voltage (V_c = 2.4 ± 0.5 V). This indicates that the ferroelectric crystalline phases are well formed in the P(VDF–TrFE) nanodots. Additionally, we observed that the hysteresis loops were horizontally shifted due to the work function (Φ) difference between the Pt-coated tip (Φ_{Pt} = 5.65 eV) and the bottom electrodes (Φ_{Au} = 5.1 eV), and the polarization offset or non-switchable dipoles.

CONCLUSIONS

In conclusion, we have successfully fabricated P(VDF–TrFE) nanodots using the simple route of spin coating and post annealing. The formation mechanism of such nanodots might involve the dewetting of the P(VDF–TrFE) thin films. We found that the initial film thickness would play an important role in the formation of P(VDF–TrFE) nanodots and that there was a critical initial film thickness (t < 24.03 ± 3.5 nm) required for the formation of the nanostructures. Uniform P(VDF–TrFE) nanodots have higher contents of the β-phase, over 60%, compared with the β-phase contents, 51%, for the 900 nm-thick tape-cast P(VDF–TrFE) films, and showed excellent piezoelectric properties, such as a remnant d_{33} value of 18.1 ± 3.3 pm/V and a coercive voltage of 2.4 ± 0.5V. This offers our rationale for a great promise in non-volatile memories, infrared imaging arrays, pressure sensor arrays and artificial skin applications. We are currently exploring self-polarization phenomena and visualization of three-dimensional dipole configuration in such nanodots using angle-resolved PFM (AR-PFM).

Table 1. Summary of the fraction of all-*trans* sequences in the P(VDF–TrFE) nanodots

Initial film thickness	F(β)
24.03 ± 3.5 nm	54.8 %
17.93 ± 2.0 nm	53.5 %
10.45 ± 1.4 nm	60.3 %

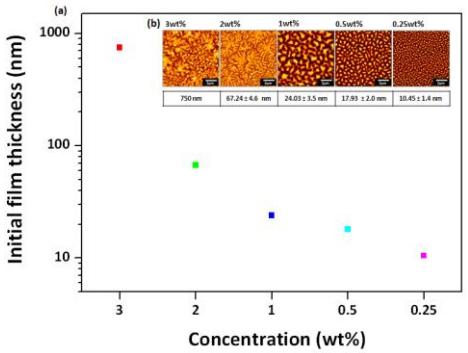

Figure 1. (a) The initial film thickness of the P(VDF–TrFE) films before annealing as a function of concentration in the range 3 wt% to 0.25 wt%. **(b)** AFM images of the P(VDF- TrFE) films made with different concentrations of P(VDF- TrFE) solution after annealing at 150 ℃.

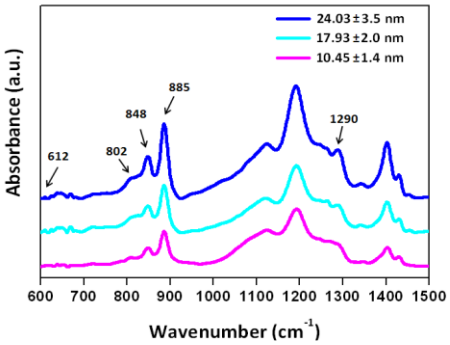

Figure 2. FT-IR spectra of the P(VDF–TrFE) nanodots obtained from (a) 24.03 ± 3.5 nm, (b) 17.93 ± 2.0 nm and (c) 10.45 ± 1.4 nm thick P(VDF–TrFE) films.

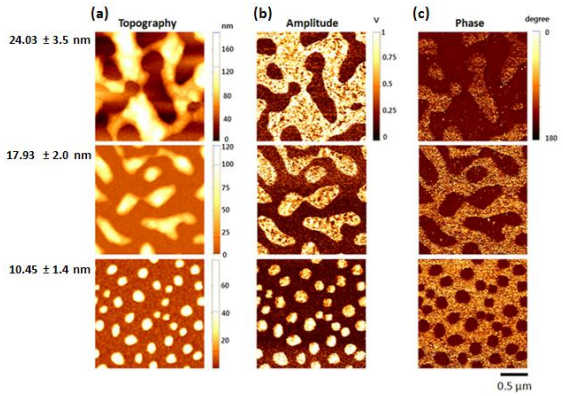

Figure 3. (a) Topological, (b) piezoelectric amplitude and (c) phase images of the self-assembled P(VDF TrFE) nanodots with initial film thicknesses of (top) 24.03 ± 3.5 nm, (middle), 17.93 ± 2.0 nm and (bottom) 10.45 ± 1.4 nm.

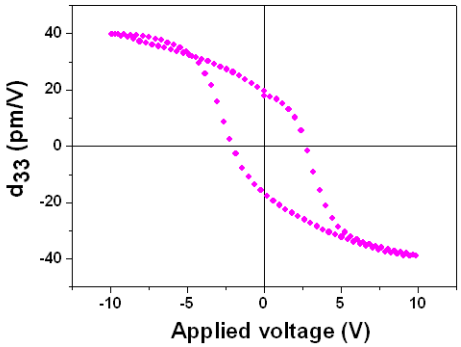

Figure 4. Piezoresponse hysteresis loops of P(VDF TrFE) nanodots.

REFERENCES

[1] Bühlmann, S, "Size effect in mesoscopic epitaxial ferroelectric structures:Increase of piezoelectric response with decreasing feature size", Appl. Phys. Lett., vol. 80, pp. 3195-3197, 2002.

[2] Nagarajan, V., "Dynamics of ferroelastic domains in ferroelectric thin films", Nat. Mater. vol. 2, pp.43-47, 2003.

[3] Nonomura, H., "Structural control of self-assembled PbTiO3 nanoislands fabricated by metalorganic chemical vapor deposition", Appl. Phys. Lett., vol. 86, 163106, 2005.

[4] Fang, J. R., "Nanoimprint of ordered ferro/piezoelectric P(VDF-TrFE) nanostructures", Micro. Eng. Article in press. 2011.

[5] Sun, Y. S., "Crystalline Polymers in Nanoscale 1D Spatial Confinement", Macromolecules, vol. 39, pp. 5782-5788, 2006.

[6] Alexe, M. "Patterning and switching of nanosize ferroelectric memory cells"Appl. Phys. Lett., vol. 75, pp. 1793-1795, 1999.

[7] Stanishevsky, A., "Radiation damage and its recovery in focused ion beam fabricated ferroelectric capacitors", J. Appl. Phys., vol. 92, pp. 3275-3278, 2002.

[8] Alexe, M., "Switching properties of self-assembled ferroelectric memory cells", Appl. Phys. Lett., vol. 75, pp. 1158-1160, 1999.

[9] Bai, M. "Ferroelectric nanomesa formation from polymer Langmuir–Blodgett films", Appl. Phys. Lett., Vol. 85, pp. 3528-3530, 2004.

[10] Zhu, G. D. "Fabrication of submicrometer- to micrometer-scale ferroelectric copolymer particles by solution mixture method", Thin solid films, vol. 517, pp. 5734-5738, 2009.

[11] Hu, Z., " Regular arrays of highly ordered ferroelectric polymer nanostructures for non-volatile low-voltage memories", Nat. Mater. vol. 8, pp. 62-67, 2008.

[12] Lee, W. " Individually addressable epitaxial ferroelectric nanocapacitor arrays with near Tb inch22 density",Nat. Nanotech. , vol. 3, pp. 402-407, 2008.

[13] Guarini, K. W., " Process integration of self-assembled polymer templates into silicon Nanofabrication", J. Vac. Sci. Technol. B, vol. 20, pp. 2788-2792, 2002.

[14] Shin, K. "A Simple Route to Metal Nanodots and Nanoporous Metal Films", Nano Lett., vol. 2, pp. 933-936, 2002.

[15] Sun, C. L. " Fabrication and characterization of Ni/P„VDF-TrFE… nanoscaled coaxial cables", Appl. Phys. Lett., vol. 90, pp. 253107, 2007.

[16] Zhang, Q. M. "Giant Electrostriction and Relaxor Ferroelectric Behavior in Electron-Irradiated Poly(vinylidenefluoride-trifluoroethylene) Copolymer", Science, vol. 280, pp. 2101, 1998.

[17] Nguyen, C. A., " Enhanced organic ferroelectric field effect transistor characteristics with strained poly(vinylidene fluoride-trifluoroethylene) dielectric", vol. 9, pp. 1087, 2008.

[18] Park, Y. J. "Ordered Ferroelectric PVDF-TrFE Thin Films by High Throughput Epitaxy for Nonvolatile Polymer Memory", Macromolecules, vol. 41, pp. 8648-8654, 2008.

[19] Choi,Y.Y, "Spin-coated ultrathin poly(vinylidene fluoride-co-trifluoroethylene) films for flexible and transparent electronics", J. Mater. Chem., vol. 21, pp. 5057-5061, 2011.